

Charge carrier transport mechanism in combustion synthesized PrAlO₃ perovskite

Saji S K^{1*}, R Radhakrishnan², Jeyasingh T¹, Vinodkumar R¹, Shibu M. Eappen³
P R Sobhana Wariar¹

¹Department of Physics, University College, Thiruvananthapuram, 695 034, India

²Department of Theoretical Physics, University of Madras, 600025, India

³STIC, Cochin University of Science and Technology, Cochin, 682 022, India

*Corresponding author

DOI: 10.5185/amp.2018/7023

www.vbripress.com/amp

Abstract

PrAlO₃ perovskite material was prepared by solution combustion technique. XRD results revealed that the material crystallizes in a rhombohedral crystal symmetry with space group R $\bar{3}c$. The ac conductivity and dielectric properties of the sintered pellet of the sample have been investigated in the frequency range 1Hz to 1MHz for a wide range of temperatures. The experimental results indicate that the ac conductivity $\sigma_{ac}(\omega)$, dielectric constant (ϵ') and dielectric loss (ϵ'') depends on the temperature and frequency. The ac conductivity was found to obey the power law ω^n with and the behavior of exponent n with temperature and the value of n suggest ion hopping is the charge transport mechanism in the material. The obtained results are compared to the principal theories that describe the universal dielectric response behavior. The value ϵ' and ϵ'' were found to be temperature and frequency dependent. Copyright © 2018 VBRI Press.

Keywords: Electronic ceramics, perovskite, rare earth aluminates.

Introduction

The perovskite are the most important class of metal oxides having both technological and geological importance [1]. Rare earth aluminates with perovskite structure have great interest due to their several applications in non-linear optics, memory devices, solid state lasers, solid electrolytes, chemical sensors, dielectric resonators etc. apart from the academic point of view due to physical properties they exhibits [2,3].

The ideal ABO₃-type perovskite structure has cubic (Pm $\bar{3}m$) symmetry, consisting of a framework of corner-sharing BO₃ octahedra with the A-type cation in each resulting cuboctahedral interstice. The majority of ABO₃ perovskites are not cubic; rather, rotation or tilting of the BO₃ octahedra provides structural flexibility, and a series of distorted structures exist. The most commonly observed distorted structures for the perovskite are the orthorhombic (Pnma) and rhombohedral (R $\bar{3}c$) structures [4].

Synthesis methods greatly influence the properties of perovskite materials. Several methods such as sol-gel, co-precipitation and conventional ceramic method etc. [5-7] have been adopted for synthesis of rare perovskite oxides. In the present work, solution combustion synthesis-a novel processing route for the synthesis of PrAlO₃ is adopted using citric acid as the complexing agent and nitric acid as the reducing agent. By the use of solution combustion synthesis it is

possible to get the fine powders, with better sinterability at relatively lower temperature. Also, it is an easy and cost effective technique for the synthesis of nanostructured materials and has the advantages of homogeneous mixing of reactants at molecular level, accurate stoichiometry control and short process period. Using these novel process nanoparticles of PrAlO₃ are synthesized. Subsequently, nanopowders were consolidated using sintering process.

Experimental

Materials and method

In analogous with our previous work [8], PrAlO₃ powders were synthesized by auto-igniting combustion process, via citrate-nitrate method, using stoichiometric amounts of Pr₆O₁₁ and Al(NO₃)₃.9H₂O. As starting materials, metal oxides Pr₆O₁₁ was dissolved in concentrated nitric acid Al(NO₃)₃.9H₂O in de-ionized water and mixed to form an aqueous solution. Proper amount of citric acid was added into the solution containing Pr³⁺ and Al³⁺ ions in maintaining citric acid to cation ratio at unity. The solution acidity was finally adjusted by adding suitable amount of ammonium hydroxide, considering too acidic solution prevent the complexations by the undissociated forms of citric acid, while too basic solutions promote the formation of metal hydroxides. The solution containing the complex precursor at neutral pH was heated on a hot plate to

about 250^o C in a ventilated fume hood. The solution boiled on heating, which underwent dehydration and decomposition leading to a thick gel. The gel slowly foamed, swelled and finally self- ignited on hot plate upon persistent heating resulting in a fluffy and voluminous dark gray powder (ash). This as synthesized powder was ground with pestle mortar and calcinated at a temperature of 1000^oC for 4 hours in air with heating and cooling rate of 5^oC/minute to remove the carbonaceous residues and to get the desired phase formation.

The calcinated powder then grounded and mixed with PVA which act as binder and pressed into cylindrical pellets by using hydraulic press with 350 MPa pressure for 5 minutes. The optimum sintering temperature was determined by sintering the compacted specimens at different temperatures in the range 1200 - 1600^oC for duration of 4h. The maximum density was obtained at 1400^oC for 4h. The bulk density of the sintered pellet was measured using the Archimedes method. The sintered specimens attained a density 97% of its theoretical value. The sintered pellets were then used for various structural and electrical measurements.

Characterizations

The single phase formation of polycrystalline PrAlO₃ perovskite was confirmed by X-ray diffraction studies. XRD analysis was performed with a X'pert Pro Bruker D-8 diffractometer with CuK_α radiation ($\lambda = 0.15418$ nm). Data were collected with steps of 0.017^o(2 θ) by varying angle from 10^o to 90^o. HR-SEM images of thermally etched surface of sintered pellets of the samples were taken on a scanning electron microscope (F E I Quanta FEG 200 - High Resolution Scanning Electron Microscope) while the elemental composition of the sample were studied by energy dispersive X-ray spectrometry (EDX). The dielectric measurements were done on the pellets as a function of frequency at various temperatures using NOVO-CONTROL (Alpha-A) high-performance frequency analyzer. Electrical contact was made on both sides of the pellets using silver coating for ohmic contact. The sample was mounted in a sample holder between two parallel electrodes, forming a capacitor. Proper shielding of the sample holder was done in order to minimize the noise disturbance.

Results and discussion

Phase analysis using X-ray diffraction

XRD pattern of PrAlO₃ powder specimen calcinated at 1000C is shown in **Fig. 1**. The X-ray diffraction (XRD) patterns of calcinated combustion powder perovskite showed the formation of PrAlO₃ perovskite rhombohedral crystal structure with the R $\bar{3}c$ space group, which is consistent with the powder diffraction file of JCPDS card no.29-0076. The patterns showed

the absence of other impurity phase. The crystallite size was estimated using Debye Scherrer's formula,

$$D = \frac{K\lambda}{\beta \cos\theta} \quad (1)$$

where, the constant K is taken as 0.9, λ is the wavelength of X-ray used and β is the full width at half maximum of the diffraction at 2 θ . The average crystallite sizes of all samples are found to be in the range of 30-70nm.

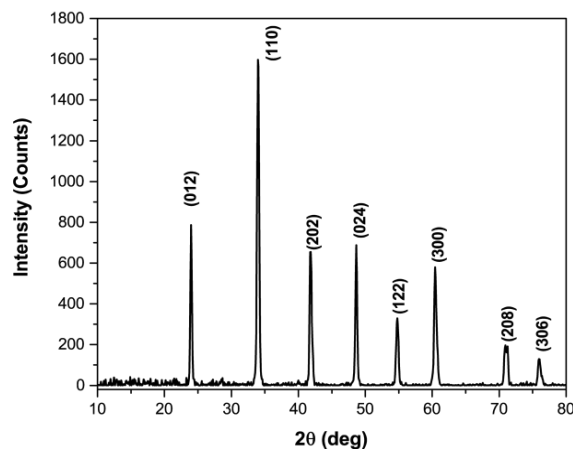


Fig. 1. XRD pattern for PrAlO₃

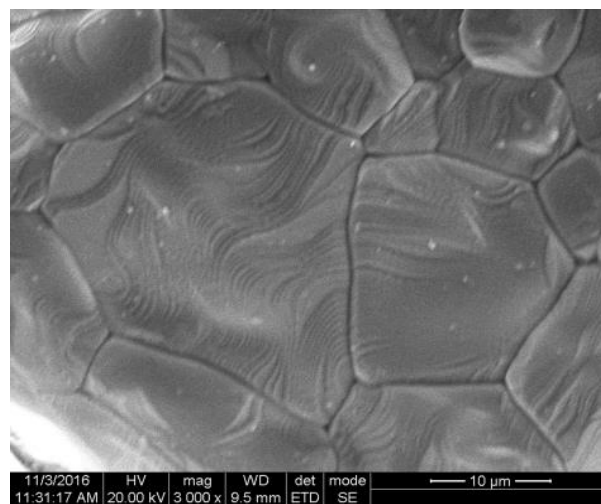


Fig. 2. HR-SEM micrograph for PrAlO₃

SEM and EDAX analysis

The surface morphology of the sintered pellet was inspected by field emission scanning electron microscopy. **Fig. 2** shows the HR-SEM micrographs for PrAlO₃ samples depicting well defined grains with sharp grain boundaries. The grain size of the samples was found to be in the range 350-500 nm.

The EDAX results obtained in the sintered specimens of PrAlO₃ depicted in the **Fig. 3**. Only the peaks corresponding to Pr, Al and O, as detected by EDAX on the sample surface and no impurity peaks are observed. The inserted table in **Fig. 3** shows the measured elemental composition of the sample surface.

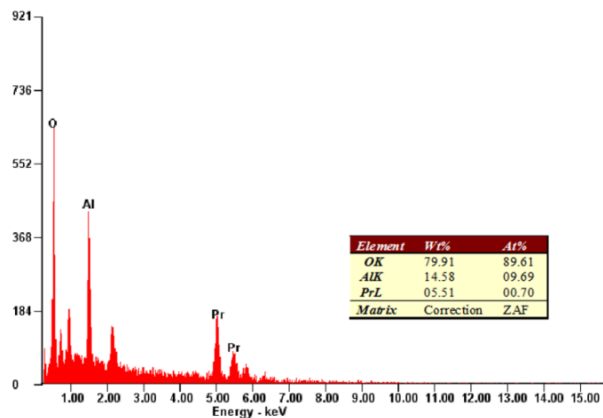


Fig. 3. EDAX spectra for PrAlO₃

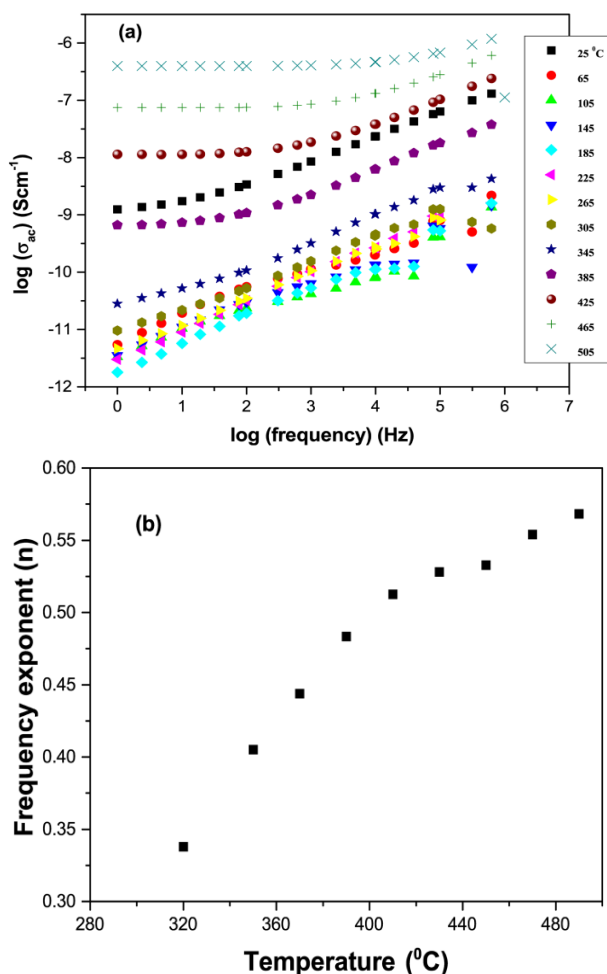


Fig. 4. (a) Frequency response of ac conductivity and (b) variation of power exponent with temperature.

Dielectric properties study

The dependence of real part of permittivity of PrAlO₃ as a function of frequency in the range 1Hz-1M Hz as observed in Fig. 4(a) shows a dispersive behavior particularly in the low frequency region. This behavior can be explained in terms of Maxwell-Wagner type of interfacial polarization in accordance with Koop’s phenomenological theory [9]. The low frequency dispersion of real permittivity ca grains and be

attributed to the grain boundary effects. The grains are known to be conducting while the grain boundaries are highly resistive. The main mode of conduction in perovskite oxide is the ion hopping between the dislocations and oxygen vacancies. In the present case, the high resistive or non-conductive grain boundaries block the mobile charge carries and inhibit charge migration resulting to piling up of charges at the grain boundaries thereby causing polarization. At low frequencies of an applied field, a net oscillation of charge carriers between occurs producing a large capacitance and hence a large dielectric constant, as has been observed. However, as the frequency of the applied field increases, the charge carriers reverse their direction of motion more often and the probability of charges reaching the grain boundaries decreases and as a result the polarization decreases. This leads to the decrease in the real part of dielectric permittivity. At higher frequencies of the applied field, hopping motion of charge carriers could not follow the frequencies of the alternating field, and therefore a low and constant value of dielectric permittivity is expected, and has been observed.

The variation of imaginary part of dielectric constant (dielectric loss) as a function of frequency in the range 1Hz-1MHz is depicted in Fig. 4(b). It can be observed that the dielectric loss decreases continuously with increasing frequency. No loss peak is observed in the frequency range of study. The decrease of dielectric loss can be explained in accordance with Koop’s phenomenological model [10]. As the frequency of the applied field is increases, the hopping frequency of charge carriers cannot follow the frequency of the alternating field and become independent of it and as a result the value of dielectric loss decreases [11].

Ac conductivity study

Frequency dependent ac conductivity (σ_{ac}) at various temperatures for PrAlO₃ ceramics is plotted in Fig. 3(a). The conductivity increases with increasing frequency and increasing temperatures. The conductivity curve shows dispersion in the low frequency region. This type of trend in conductivity is very similar to that in ionic conducting ceramics [12].

The ac conductivity of any dielectric or semiconducting material can be expressed in terms of Jonscher’s power law [13]:

$$\sigma(\omega) = \sigma_0 + A\omega^n \tag{2}$$

where ω is angular frequency, n is a constant ($0 < n < 1$) and σ_0 is the low-frequency conductivity. The values of exponent n are obtained by fitting ac conductivity data using above equation. The value of found to 'n' increases with increase in temperature and is depicted in Fig 3(b). At all temperature under observation the values of n found to be less than unity further suggests ion hopping conduction in the material.

Conclusion

The frequency dependent dielectric dispersion of perovskite PrAlO_3 ceramics were prepared by solution combustion technique and is investigated in the frequency range at 1 Hz to 1MHz at different temperatures. The crystal structures of ceramics determined by powder X-ray diffraction shows rhombohedral phase at room temperature. The variation of dielectric constant and dielectric loss may be attributed to hopping of trapped charge carriers, which resulted in an extra dielectric response in addition to the dipole response. The behavior of exponent n with temperature confirms hopping type charge transport in the material.

Acknowledgements

Saji S K acknowledges University Grants Commission (UGC), India for the award of teacher fellowship under the faculty development programme. We also thank Dr. Archana Lakhani and Dr. A M Awasthi, UGC-DAE Consortium for Scientific Research, Indore for the dielectric measurement.

References

1. Kennedy, B.J., Vogt, T., Martin, C.D., Parise, J.B. and Hriljac, J.A., *Chemistry of Materials*, **2002**, *14*, 2644.
DOI: [10.1021/cm0116976](https://doi.org/10.1021/cm0116976)
2. Vasylechko, L., Senyshyn, A. and Bismayer, U., **2009**, *39*, 295.
DOI: [10.1016/S0168-1273\(08\)00002-0](https://doi.org/10.1016/S0168-1273(08)00002-0)
3. Jancar, B., Suvorov, D., Valant, M. and Drazic, G., *Journal of the European Ceramic Society*, **2003**, *23*, 1391.
DOI: [10.1016/S0955-2219\(02\)00359-X](https://doi.org/10.1016/S0955-2219(02)00359-X)
4. Kennedy, B.J., Vogt, T., Martin, C.D., Parise, J.B. and Hriljac, J.A., *Chemistry of Materials*, **2002**, *14*, 2644.
DOI: [10.1021/cm0116976](https://doi.org/10.1021/cm0116976)
5. Rabuffetti, F.A., Lee, J.S. and Brutchey, R.L., *Advanced Materials*, **2012**, *24*, 1434.
DOI: [10.1002/adma.201104645](https://doi.org/10.1002/adma.201104645)
6. Haron, W., Wisitsoraat, A. and Wongnawa, S., *Ceramics International*, **2017**.
DOI: [10.1016/j.ceramint.2017.01.013](https://doi.org/10.1016/j.ceramint.2017.01.013)
7. Sánchez-Rodríguez, D., Wada, H., Yamaguchi, S., Farjas, J. and Yahiro, H., *ACyano Ceramics International*, **2017**, *43*, 3156.
DOI: [10.1016/j.ceramint.2016.11.134](https://doi.org/10.1016/j.ceramint.2016.11.134)
8. Saji, S.K., Vinodkumar, R., Eappen, S.M. and Wariar, P.S., *Materials Chemistry and Physics*, **2017**, *193*, 189.
DOI: [10.1016/j.matchemphys.2017.02.024](https://doi.org/10.1016/j.matchemphys.2017.02.024)
9. Liu, J., Duan, C.G., Yin, W.G., Mei, W.N., Smith, R.W. and Hardy, J.R., *Physical Review B*, **2004**, *70*, 144106.
DOI: [10.1103/PhysRevB.70.144106](https://doi.org/10.1103/PhysRevB.70.144106)
10. Koons, C.G., *Physical Review*, **1951**, *83*, 121.
DOI: [10.1103/PhysRev.83.121](https://doi.org/10.1103/PhysRev.83.121)
DOI: [10.1111/j.1151-2916.1990.tb06430.x](https://doi.org/10.1111/j.1151-2916.1990.tb06430.x)
11. Jonscher, A.K., *IEEE Transactions on Electrical Insulation*, **1992**, *27*, 407.
DOI: [10.1109/14.142701](https://doi.org/10.1109/14.142701)
12. Jonscher, A.K., *Thin Solid Films*, **1983**, *100*, 329.
DOI: [10.1016/0040-6090\(83\)90157-8](https://doi.org/10.1016/0040-6090(83)90157-8)
13. Jonscher, A.K., *Nature*, **1975**, *253*, 717.
DOI: [10.1038/253717a0](https://doi.org/10.1038/253717a0)